



Minerva Access is the Institutional Repository of The University of Melbourne

Author/s:

Nguyen, THO;McAuley, JL;Kim, Y;Zheng, MZM;Gherardin, NA;Godfrey, DI;Purcell, DFJ;Sullivan, LC;Westall, GP;Reading, PC;Kedzierska, K;Wakim, LM

Title:

Influenza, but not SARS-CoV-2, infection induces a rapid interferon response that wanes with age and diminished tissue-resident memory CD8+ T cells

Date:

2021-01-01

Citation:

Nguyen, T. H. O., McAuley, J. L., Kim, Y., Zheng, M. Z. M., Gherardin, N. A., Godfrey, D. I., Purcell, D. F. J., Sullivan, L. C., Westall, G. P., Reading, P. C., Kedzierska, K. & Wakim, L. M. (2021). Influenza, but not SARS-CoV-2, infection induces a rapid interferon response that wanes with age and diminished tissue-resident memory CD8+ T cells. *Clinical and Translational Immunology*, 10 (1), <https://doi.org/10.1002/cti2.1242>.

Persistent Link:



<https://hdl.handle.net/11343/272853>

License:

[CC BY-NC-ND](#)

ORIGINAL ARTICLE

Influenza, but not SARS-CoV-2, infection induces a rapid interferon response that wanes with age and diminished tissue-resident memory CD8⁺ T cells

Thi HO Nguyen¹, Julie L McAuley¹, Youry Kim¹, Ming ZM Zheng¹, Nicholas A Gherardin^{1,2} , Dale I Godfrey^{1,2}, Damian FJ Purcell¹, Lucy C Sullivan^{1,3}, Glen P Westall^{3,4}, Patrick C Reading^{1,5}, Katherine Kedzierska¹  & Linda M Wakim¹

¹Department of Microbiology and Immunology, Peter Doherty Institute for Infection and Immunity, The University of Melbourne, Melbourne, VIC, Australia

²Australian Research Council Centre of Excellence for Advanced Molecular Imaging, University of Melbourne, Melbourne, VIC, Australia

³Lung Transplant Service, Alfred Hospital, Melbourne, VIC, Australia

⁴Department of Medicine, Monash University, Melbourne, VIC, Australia

⁵WHO Collaborating Centre for Reference and Research on Influenza, Victorian Infectious Diseases Reference Laboratory, Peter Doherty Institute for Infection and Immunity, Melbourne, VIC, Australia

Correspondence

LM Wakim and K Kedzierska, Department of Microbiology & Immunology, University of Melbourne, The Doherty Institute for Infection & Immunity, Level 8, 792 Elizabeth Street, Melbourne, VIC 3000, Australia.
Emails: wakim@unimelb.edu.au (LMW);
kkedz@unimelb.edu.au (KK)

Received 19 November 2020;

Revised 27 December 2020;

Accepted 28 December 2020

doi: 10.1002/cti.1242

Clinical & Translational Immunology

2021; 10: e1242

Abstract

Older individuals exhibit a diminished ability to respond to and clear respiratory pathogens and, as such, experience a higher rate of lung infections with a higher mortality rate. It is unclear why respiratory pathogens impact older people disproportionately. Using human lung tissue from donors aged 22–68 years, we assessed how the immune cell landscape in lungs changes throughout life and investigated how these immune cells respond following *in vitro* exposure to influenza virus and SARS-CoV-2, two clinically relevant respiratory viruses. While the frequency of most immune cell subsets profiled in the human lung remained stable with age, memory CD8⁺ T cells declined, with the tissue-resident memory (Trm) CD8⁺ T-cell subset being most susceptible to age-associated attrition. Infection of lung tissue with influenza virus resulted in an age-associated attenuation in the antiviral immune response, with aged donors producing less type I interferon (IFN), GM-CSF and IFN γ , the latter correlated with a reduction of IFN γ -producing memory CD8⁺ T cells. In contrast, irrespective of donor age, exposure of human lung cells to SARS-CoV-2, a pathogen for which all donors were immunologically naïve, did not trigger activation of local immune cells and did not result in the induction of an early IFN response. Our findings show that the attrition of tissue-bound pathogen-specific Trm in the lung that occurs with advanced age, or their absence in immunologically naïve individuals, results in a diminished early antiviral immune response which creates a window of opportunity for respiratory pathogens to gain a greater foothold.

Keywords: influenza, lung, resident memory T cells, SARS-CoV-2

INTRODUCTION

Globally, the population of individuals aged 65 and over is growing faster than all other age groups, and by 2050, one in six people in the world will be over the age of 65 (16%). Older individuals are highly susceptible to respiratory pathogens, and pulmonary infections in the elderly often lead to worse outcomes, prolonged hospital stays and life-threatening complications.¹ Older individuals may be more prone to exacerbated respiratory infections as a result of the systemic decline in the immune system that occurs with age (immunosenescence), which results in reduced immunological surveillance and a depressed ability to mount an appropriate immune response.^{2,3} While this systemic immunosenescence may explain, in part, why the elderly has an increased susceptibility to pulmonary infections, whether local changes in the immune cell landscape also contribute to this increased susceptibility to respiratory pathogens remains unclear. Here, we profiled how the immune cell composition in the lung changed with increased age and investigated how these changes impact the immune response following infection with influenza virus and severe acute respiratory syndrome coronavirus 2 (SARS-CoV-2), two respiratory viruses that cause exacerbated disease in the elderly. Worldwide, annual influenza epidemics are estimated to result in 250 000–500 000 deaths and up to 5 million cases of severe illness with approximately 90% of influenza-related deaths and 50–70% of influenza-related hospitalisations occurring in adults 65 years of age and older.⁴ SARS-CoV-2 originated in Wuhan, China, in late 2019 and has since caused a worldwide pandemic of coronavirus disease (COVID-19). COVID-19 has so far killed more than 1.33M people, with 80% of deaths occurring in people over the age of 65.⁵ A better understanding of the factors that predispose the elderly to lower respiratory tract infections will allow for the development of approaches that attenuate the severity of pulmonary disease in these vulnerable individuals.

To elucidate how age impacts the local antiviral immune response in the lung, we profiled the immune cell landscape in lung tissue from a cohort of 8 organ donors aged 22–68 years. We found that although most immune cell subsets

profiled remained stable with age, the frequency of memory CD8⁺ T cells, specifically the tissue-resident memory (Trm) CD8⁺ T-cell subset, waned. Infection of lung tissue with influenza virus resulted in an age-associated attenuation in the antiviral immune response that correlated with a reduction in the frequency of influenza-reactive lung Trm. In contrast, exposure of human lung cells to SARS-CoV-2, a pathogen for which all donors were immunologically naïve, did not trigger activation of local immune cells and did not result in the induction of an interferon response irrespective of donor age. Our results show that pathogen-specific CD8⁺ lung Trm are a frontline defence that exert an immediate response following virus re-exposure. The attrition of these lung Trm that occurs with advanced age, or their absence in immunologically naïve individuals, results in a diminished early antiviral response and a lost opportunity to blunt infection before the development of severe disease.

RESULTS

Decay of memory CD8⁺ T cells in the lung occurs with age

We measured the frequency of different immune cells present within human lung tissue from organ donors between the ages of 22–68 years. Lung sample preparations contained > 60% haematopoietic cells (CD45⁺) and were banked prior to December 2019 (Figure 1a). We observed no correlation in the frequency of B cells, MAIT cells, NK cells and CD4⁺ T cells and the age of the donor (Figure 1b and c), although MAIT cells appear to follow a biphasic rise then fall with age, as previously reported.^{6,7} Interestingly, the proportion of lung CD8⁺ T cells, the vast majority of which were antigen experienced (CD45RO⁺), declined in the elderly, with these cells representing ~ 21% of the total cells in lungs of donors < 50 years of age, but only ~ 7.5% of the total cells in donors > 50 years of age (Figure 1c and d). Attrition of memory CD8⁺ T cells with age appears to be most pronounced in the lung environment, as assessment of the frequency of memory CD8⁺ T cells in the blood of a cohort of non-matched donors showed that the proportion of memory CD8⁺ T cells does not wane with age (Supplementary figure 1), which is in line with our

previous studies showing a gradual increase in the size of the circulating memory CD8⁺ T-cell pool with advanced age.⁸ Assessment of the bulk CD8⁺ T-cell pool in the lung also revealed age-related changes in T-cell subset composition, with naïve T cells (CD45RA⁺CD27⁺) declining and effector memory T cells (CD45RA⁻CD27⁻) increasing with advanced age (Supplementary figure 2). Interestingly, further phenotypic profiling of lung memory CD8⁺ T cells revealed that Trm, a memory T-cell subset, identified here by the co-expression of CD69 and the integrin CD103⁹ also declined with age, with Trm representing ~48% of total memory CD8⁺ T cells in donors <50 years of age, but only ~25% of the total lymphocytes in donors >50 years of age (Figure 1e–g). The decrease in the frequency of Trm coincided with a reciprocal increase in the proportion of CD69⁻CD103⁻ memory CD8⁺ T cells (Figure 1f and g). We have previously reported CD103⁺CD69⁺ CD8⁺ Trm frequencies in another cohort of lung organ donors,⁹ and when we combine the data acquired from both cohorts, thereby increasing the sample size to 14 donors, we still see a significant negative correlation between age and Trm frequency (Supplementary figure 3, Pearson $r = -0.608$, $*P = 0.021$). Thus, the immune cell landscape in the human lung changes with advanced age, resulting in a decrease in the frequency of tissue-residing memory CD8⁺ T cells.

Upregulation of activation markers on T cells in the lung following exposure to influenza virus decreases with age

We next investigated whether the age-associated changes in the lung immune cell landscape impact the quality of the immune response mounted following exposure to influenza virus. To do this, we infected single-cell suspensions of whole lung tissues with influenza virus (H3N2, X31) at a multiplicity of infection (moi) of 1, and 24 h later measured the levels of expression markers indicative of immune cell activation, including CD38, HLA-DR, CD27, PD-1 and CD69, on both innate-like (MAIT cells and $\gamma\delta$ T cells) and conventional (CD4 and CD8) T cells. We limited our analysis here to the T-cell compartment as it was these cells that were most affected by donor age (see Figure 1). Influenza virus infection of human lung tissue caused the upregulation of expression of HLA-DR and CD69 on all T-cell subsets profiled, albeit with varying efficiencies,

and upregulated expression of CD38 on both $\gamma\delta$ T cells and CD8⁺ T cells (Figure 2a–e). Interestingly, when profiling the memory CD8⁺ T-cell pool, we observed that the level of upregulation of CD69 and HLA-DR negatively correlated with donor age (Figure 2e). We checked the proportion of the lung cells that were infected with influenza virus, as assessed by intracellular staining for the viral nucleoprotein (NP), to rule out that the observed differences in T-cell activation across age groups was a consequence of variations in infection efficiency. We found that 1–5% of lung cells stained positive for influenza virus NP, and importantly, the level of infection was not influenced by the age of the donor (Supplementary figure 4). Thus, in addition to an age-associated drop in the frequency of lung memory CD8⁺ T cells we also find that with advanced age, the bulk memory CD8⁺ T cells that are present in the lung undergo less activation following influenza virus exposure.

Exposure of lung cells to influenza virus triggers an early pro-inflammatory response that decreases with age

To determine whether the age-associated changes in the immune cell landscape in the lung impact the inflammatory profile following exposure to influenza virus, single-cell suspensions of whole lung tissue were infected *in vitro* with mouse-adapted influenza virus (H3N2, X31) at a moi of 1 and 24, and 48 h later, the level of a panel of cytokines in the supernatant was measured. Several pro-inflammatory cytokines including TNF, IL-6, IFN- λ 1, IFN- β , IL-10, IL-8 and CXCL10 were induced following exposure to influenza virus, and the amount released appeared unaffected by the age of the donor (Figure 3a). While influenza virus infection also caused the production of GM-CSF, IFN γ and IFN α , the amount of these cytokines produced at 24 and 48 h post-infection negatively correlated with the age of the donor (Figure 3a). Next, we tested whether infection with human influenza virus strains also triggered a similar inflammatory profile. To do this, single-cell suspensions of whole lung tissue were infected *in vitro* at a moi of 1 with either A/Sydney/203/2000 (H3N2) or A/Tasmania/2004/2009 (H1N1pdm09) and 24 and 48 h later, the level of infection, measured by intracellular NP staining, and the presence of GM-CSF, IFN γ and IFN α 2 in the supernatant was assessed. Similar to our

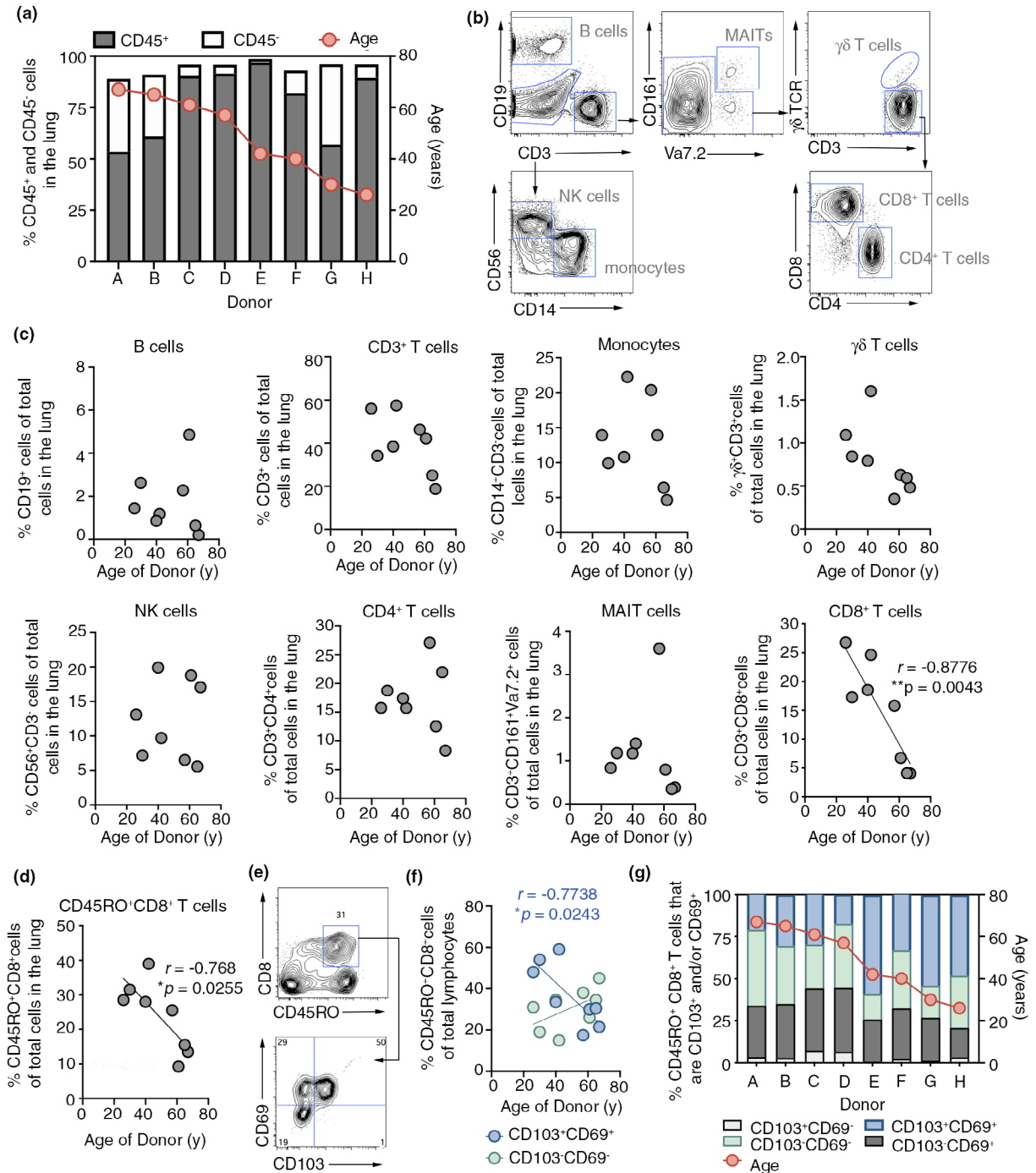


Figure 1. Age-associated decay of lung memory CD8⁺ T cells. **(a)** The proportion of CD45⁺ and CD45⁻ cells in the lung of donors. Bars represent individual donors, and symbols show the donor's age. **(b)** Representative gating strategy for identifying immune cell subsets. **(c)** The frequency of B cells (CD19⁺CD3⁻), CD3⁺ T cells (CD3⁺CD19⁻), monocytes (CD3⁺CD19⁻CD56⁺CD14⁺), $\gamma\delta$ T cells (CD3⁺CD161⁺Va7.2⁺ $\gamma\delta$ TCR⁺), NK cells (CD3⁺CD19⁻CD56⁺), CD4⁺ T cells (CD3⁺CD161⁻ $\gamma\delta$ TCR⁻CD4⁺CD8⁺), MAIT cells (CD3⁺CD161⁺Va7.2⁺) and CD8⁺ T cells (CD3⁺CD161⁻ $\gamma\delta$ TCR⁻CD4⁺CD8⁺) of total cells in the lungs plotted against age (years). **(d)** The frequency of CD45RO⁺CD8⁺ memory CD8⁺ T cells of cells in the lungs plotted against age (years). **(e)** Flow cytometry profiles depicting the level of expression of CD103 and CD69 on memory CD8⁺ T cells (CD45RO⁺CD8⁺CD3⁺) isolated from human lung. **(f)** The frequency of CD8⁺ Trm (CD3⁺CD45RO⁺CD8⁺CD103⁺CD69⁺) of total memory CD8⁺ T cells plotted against age (years). **(g)** The proportion of memory CD8⁺ T cells (CD3⁺CD45RO⁺CD8⁺) isolated from the lung that express CD103 and CD69. Bars represent individual donors. Symbols show the donor's age (years). In **c**, **d** and **f**, symbols represent individual donors, and the line represents Pearson's correlation. $*P < 0.05$; $**P < 0.01$.

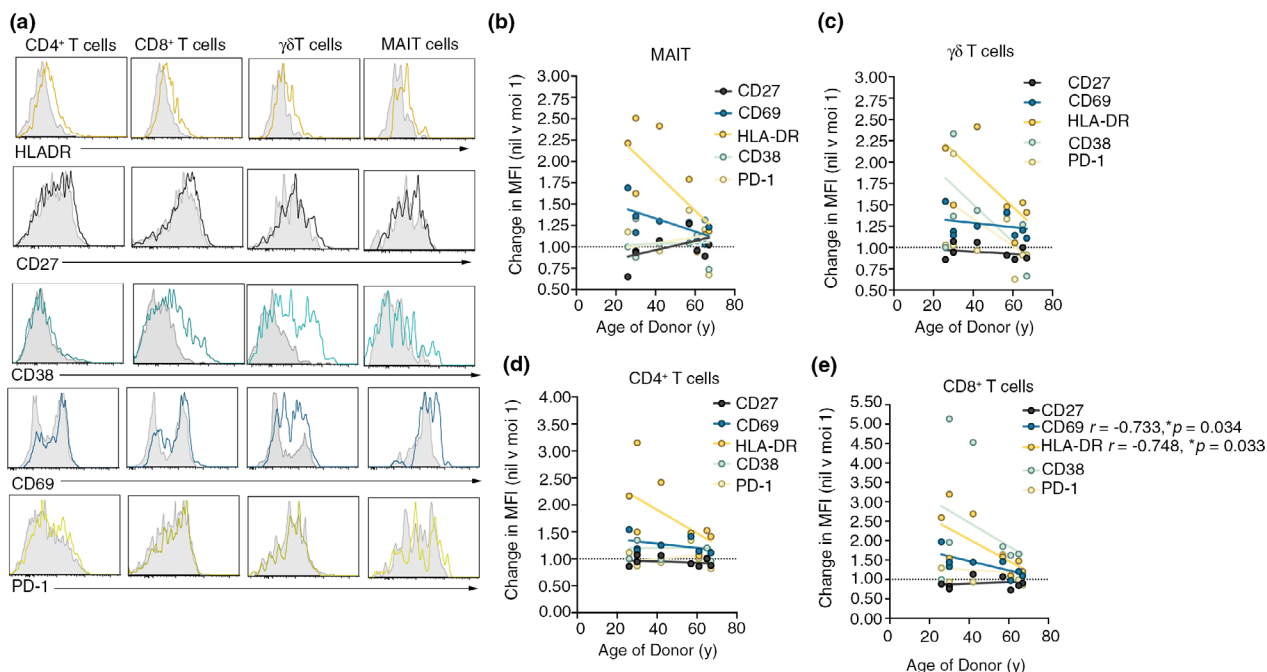


Figure 2. Upregulation of activation markers on innate and conventional T cells in the lung following exposure to influenza virus decreases with age. **(a–e)** Lung cells were infected with influenza virus (X31) at moi of 1, and expression of HLA-DR, CD27, CD38, CD69 and PD-1 on memory CD4⁺ T cells, memory CD8⁺ T cells, γδ T cells and MAIT cells was measured 24 h later. **(a)** Representative histograms show the expression level of activation markers post-influenza virus exposure on specific immune cell subsets. Grey histograms show expression on cells from uninfected cultures. **(b–e)** Fold change in mean fluorescence intensity (MFI) of CD27, CD69, HLA-DR, CD38 and PD-1 on **(b)** MAIT cells, **(c)** γδ T cells, **(d)** memory CD4⁺ T cells and **(e)** memory CD8⁺ T cells present in influenza virus-infected lung tissue relative to the expression on cells in uninfected control cultures (Nil) plotted against age (years). Symbols represent individual donors, and the line represents Pearson’s correlation. * $P < 0.05$.

earlier results, we did not observe any age-associated impact on the ability of human influenza viruses to infect lung tissue, with 2.6–12% of lung cells staining NP⁺ following infection with A/Sydney/203/2000 and 1.8–6.2% of lung cells staining NP⁺ following infection with A/Tasmania/2004/2009 (Supplementary figure 5a). In alignment with our observations following infection of human lung tissue with the mouse-adapted X31 virus, we again observed that aged donors produce less IFN α 2, GM-CSF and IFN γ following infection with the human influenza isolates (Supplementary figure 5b–e). To gain insight into the cellular source of these cytokines, we repeated the experiment and this time added brefeldin A to the culture to trap cytokines intracellularly and profiled various immune cells including CD8⁺ T cells, CD4⁺ T cells, MAIT cells, NK cells and γδ T cells at 18 h post-infection for the production of IFN γ and GM-CSF. Negligible levels of GM-CSF were detected in all immune cells profiled which suggests that another cell type not

profiled in this assay is likely the source of this inflammatory cytokine (Figure 3b). Assessment of IFN γ production revealed that memory CD8⁺ T cells were the main source and consistent with our earlier findings, the proportion of CD8⁺ memory T cells making IFN γ in response to influenza virus infection waned with age (Figure 3b and c). Collectively, these results suggest that following infection with influenza virus, lung tissue from aged donors produces less IFN α , GM-CSF and IFN γ , the latter perhaps attributed by the reduction in IFN γ -producing memory CD8⁺ T cells.

Decay of influenza virus-specific tissue-resident memory T cell occurs with age

The diminished activation and IFN γ production by memory CD8⁺ T cells in the lungs of aged donors following exposure to influenza virus may be explained by a loss of influenza virus-reactive memory CD8⁺ T cells in this tissue. To investigate

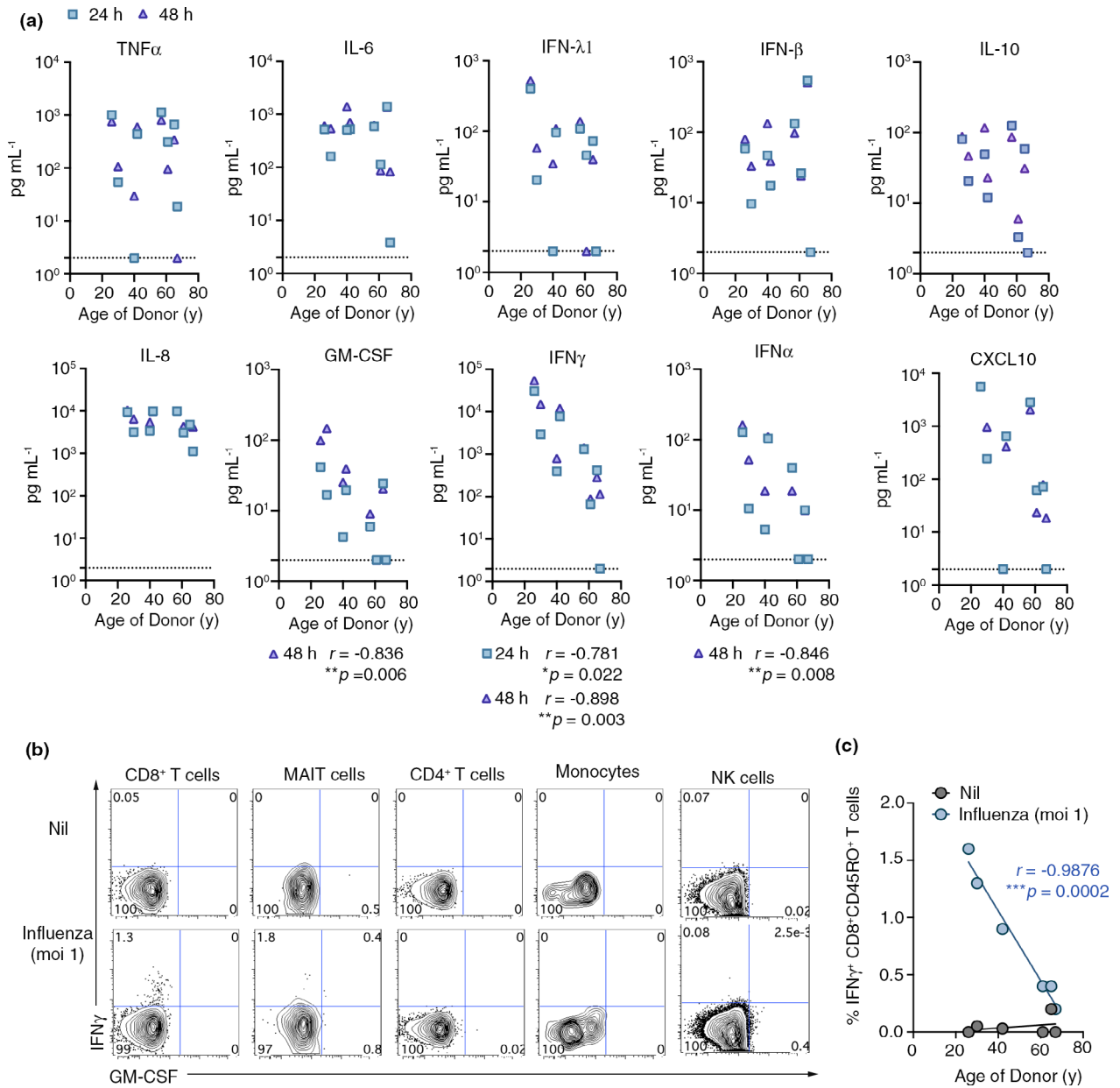


Figure 3. Exposure of lung cells to influenza virus triggers an early pro-inflammatory response that decreases with age. **(a)** Lung cells were infected with influenza virus (X31) at moi of 1, and the levels of a panel of inflammatory cytokines released into the supernatant at 24 and 48 h were measured using a cytometric bead array. Graphs depict the amount (pg mL⁻¹) of inflammatory cytokine plotted against age (years). Symbols represent individual donors, and the dotted line represents the limit of detection (r = Pearson’s correlation). **(b, c)** Lung cells were infected with influenza virus (X31) at moi of 1 in the presence of brefeldin A, and the percentage of different immune cells generating intracellular IFN γ and GM-CSF was measured 18 h later. **(b)** Representative flow cytometry profile staining for GM-CSF and IFN γ on immune cell subsets with or without (Nil) virus infection. **(c)** The graph depicts the proportion of IFN γ -producing memory CD8⁺ T cells with or without (Nil) virus infection plotted against age (years). Symbols represent individual donors, and the line represents Pearson’s correlation. $*P < 0.05$; $**P < 0.01$; $***P < 0.001$.

this further, we measured the frequency of influenza-specific memory CD8⁺ T cells in lung of donors using a panel of HLA-peptide tetrameric complexes and enumerated the influenza virus-

specific cells by flow cytometry. Within our cohort, we identified 7 donors with HLA types for which HLA tetramers loaded with influenza immunodominant epitopes were available. These

included donors who were HLA-A1, HLA-A2 and HLA-A3.¹⁰ The proportion of influenza-specific (tetramer positive) CD8⁺ T cells of the total memory CD8⁺ T-cell pool across the donors ranged from 0.4% to 8.6%, and similar to our previously reported studies,^{9,11} we observed no correlation between the size of the lung influenza-specific memory CD8⁺ T-cell pool and donor age (Figure 4a and b). These data suggest that the difference in memory CD8⁺ T-cell activation observed in aged donors following exposure to influenza virus is not simply because of a reduction in influenza virus-specific CD8⁺ memory T cells. Interestingly, while the overall frequency of influenza-specific lung memory CD8⁺ T cells was not affected by donor age, further inspection of this virus-specific memory T-cell pool did reveal age-related changes in memory T-cell subset composition. Consistent with our observed changes in the bulk memory CD8⁺ T-cell compartment, we found the proportion of CD103⁺CD69⁺ influenza-specific CD8⁺ Trm cells declined with age (Figure 4c) and this coincided with a reciprocal increase in the proportion of CD69⁻CD103⁻ memory CD8⁺ T cells (Figure 4d and e). These results highlight the local resident memory CD8⁺ T-cell compartment in the lung declines with age, and this may, in part, impact the size and quality of the early inflammatory response evoked following virus exposure.

T cells in the lung fail to upregulate activation markers following exposure to SARS-CoV-2

We next investigated how the immune cells in the lung react following exposure to SARS-CoV-2, another respiratory pathogen which causes severe disease in the elderly. As all lung tissue was stored prior to the emergence of SARS-CoV-2, all donors will be immunologically naïve. Single-cell suspensions of whole lung tissue were infected with SARS-CoV-2 at a moi of 1, and 24 and 48 h later, the activation status of both innate-like (or unconventional) and conventional T cells was measured by assessing the expression of HLA-DR, CD38, CD27, PD-1 and CD69. In parallel, as a positive control, we also infected cells with influenza virus. At 24 h post-SARS-CoV-2 infection, irrespective of the donor age, we did not observe upregulation of any activation marker on any T-cell subset profiled (data not shown), a phenotype that was conserved at 48 h post-SARS-CoV-2

infection (Figure 5a–d). In contrast, and consistent with our earlier 24-h experiments, infection of the lung tissue with influenza virus for 48 h triggered both innate and conventional T-cell activation as measured by upregulation of HLA-DR and CD69 expression, and the upregulation of CD38 expression on both $\gamma\delta$ T cells and CD8⁺ T cells (Figure 5a–d). The inability of SARS-CoV-2 infection to trigger immune cell activation was not because the virus was unable to infect these lung cells as assessment of viral RNA by RT-qPCR at 1, 24 and 48 h post-infection confirmed the presence of an increasing level of virus in all infected samples (Figure 5e–g). Moreover, utilising a recombinant, fluorescently tagged SARS-CoV-2 RBD-dimer protein to identify angiotensin-converting enzyme 2 (ACE2), a transmembrane protein that serves as a receptor for entry of SARS-CoV-2 into host cells, we show that CD14⁺ cells in the human lungs can bind the RBD-dimer and the level of attachment does not appear to be influenced by donor age (Supplementary figure 6). To assess whether SARS-CoV-2 infection of the lung tissue triggers the release of pro-inflammatory molecules, the levels of a panel of cytokines released into the supernatants were measured. Of interest, while influenza virus infection triggered the production of type I, II and III interferon, infection with SARS-CoV-2 did not evoke production of any of these interferons (Figure 6). Collectively, these results show that irrespective of donor age, exposure of human lung cells to SARS-CoV-2 does not trigger the activation of local immune cells and does not result in the induction of an early interferon response.

DISCUSSION

Older individuals exhibit a diminished ability to respond to and clear respiratory infections. To gain insight into the increased susceptibility of the elderly to respiratory infection, we profiled the immune cell composition in the lung with increased age and investigated how these changes impacts the immune response following exposure to influenza virus and SARS-CoV-2. We found that the frequency of lung Trm wanes with advanced age and that this results in a diminished early antiviral immune response.

Trm are a non-recirculating, self-sustaining class of memory CD8⁺ T cells lodged within a variety of peripheral tissues that play a critical role in local

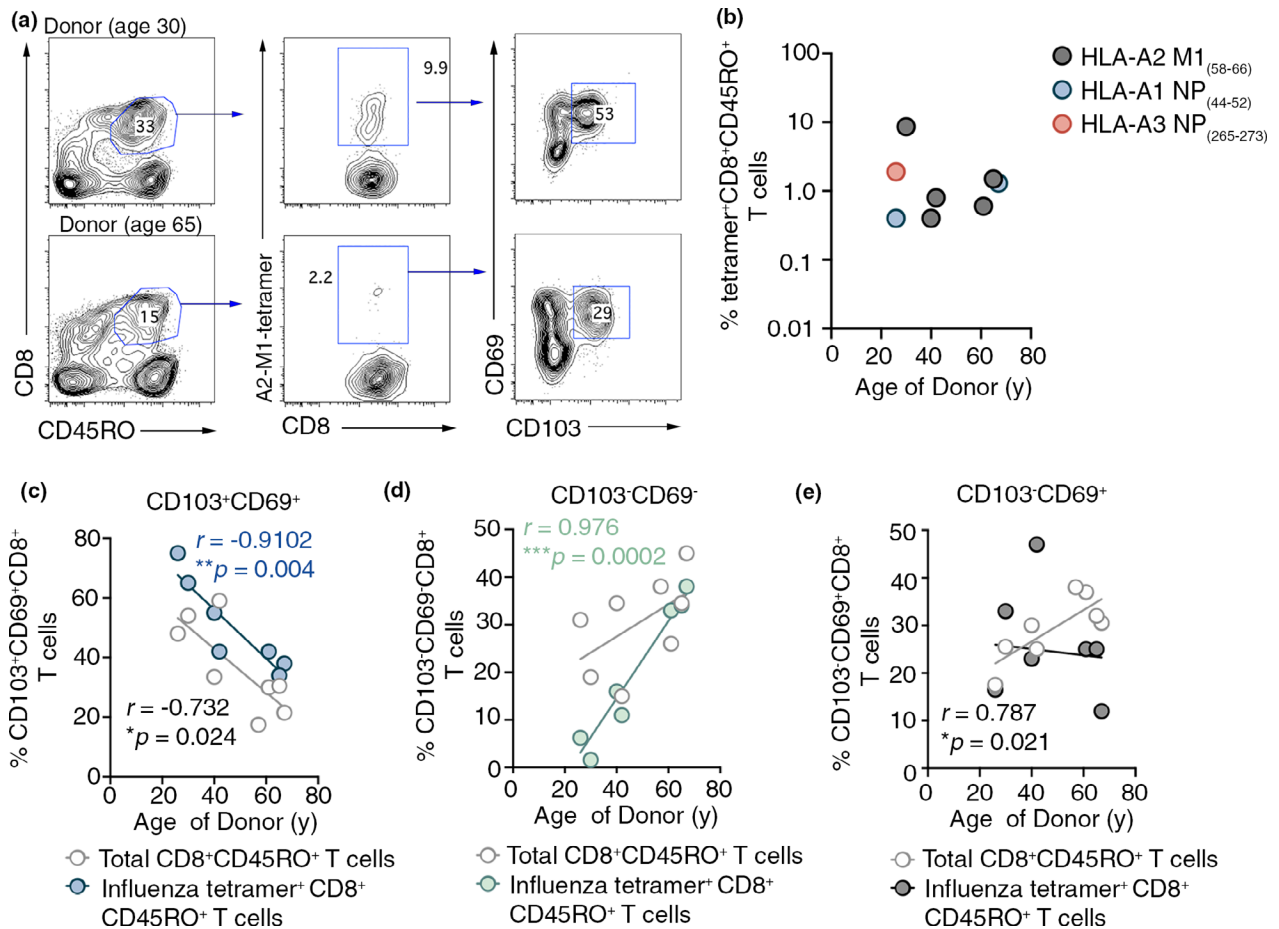


Figure 4. Decay of influenza virus-specific CD8⁺ Trm occurs with age. **(a)** Representative flow cytometry staining assessing the expression of CD103 and CD69 on HLA-A2-M1₅₈₋₆₆-specific CD8⁺ T cells isolated from lung tissue of two donors. **(b)** The percentages of influenza tetramer⁺CD8⁺ T cells of the total memory CD8⁺ T-cell pool (CD3⁺CD8⁺CD45RO⁺) in the lungs of donors plotted against age (years). **(c–e)** The frequency of total memory CD8⁺ T cells and influenza tetramer⁺ memory CD8⁺ T cells that are **(c)** CD103⁺CD69⁺ Trm, **(d)** CD103⁻CD69⁻ and **(e)** CD103⁻CD69⁺ plotted against age (years). Symbols represent individual donors, and the line represents Pearson's correlation. * $P < 0.05$; ** $P < 0.01$; *** $P < 0.001$.

immune protection. During a localised infection, Trm serve as frontline responders, tasked with orchestrating local protective immune responses.¹² CD8⁺ Trm act rapidly following pathogen encounter, undergoing *in situ* expansion^{13–15} and gaining cytotoxic activity. Moreover, these Trm also promote an antiviral environment in the tissue by releasing cytokines that trigger the activation and recruitment of other immune cells to the site of infection,^{16–18} as well as evoking the expression of antiviral proteins on neighbouring cells.¹⁹ The human lung harbours a large population of CD8⁺ Trm²⁰ that are highly proliferative,⁹ poised for rapid polyfunctional responsiveness²¹ and are composed of a diverse TCR $\alpha\beta$ repertoire, with no indication of clonal

skewing or TCR repertoire narrowing.^{9,20} Here, we find that the pool of CD8⁺ Trm in the lung undergoes age-associated attrition. While CD103⁺CD69⁺ Trm represent approximately 48% of total memory CD8⁺ T cells in the lungs of donors aged < 50 years, they only account for approximately 25% of the total memory CD8⁺ T cells in the lungs of donors aged > 50 years. Mouse models clearly show that lung Trm, unlike their counterparts in other tissues, decay over time.^{22,23} While it is still unclear why lung Trm wane with time, several factors within the microenvironment of the lung, for example oxygen tension and the presence of immunosuppressive agents (i.e. Tregs and IL-10), have been proposed to influence the longevity of

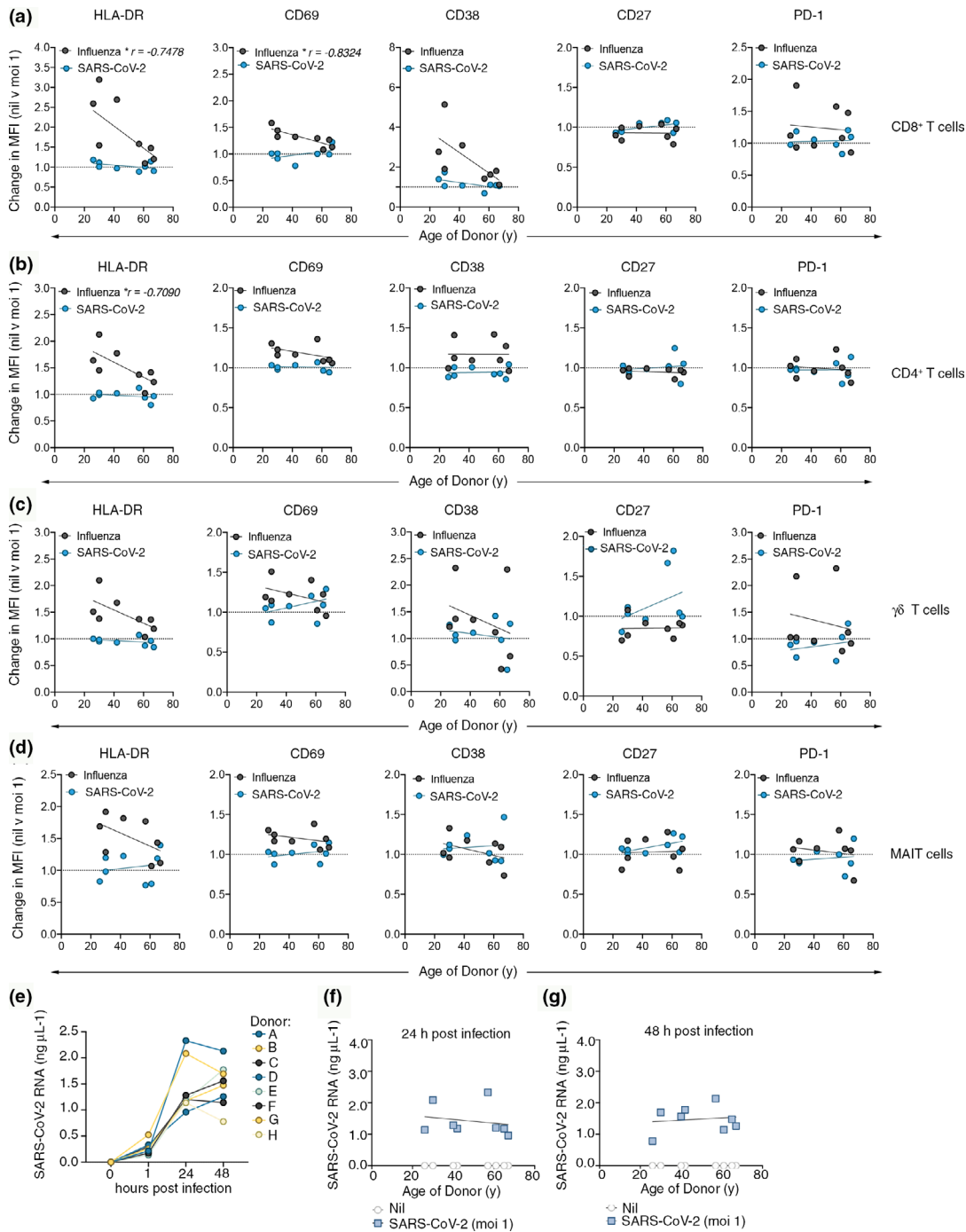


Figure 5. Innate-like and conventional T cells in the lung fail to upregulate activation markers following exposure to SARS-CoV-2. **(a–d)** Cells from whole lung tissue were infected with either influenza virus (X31) or SARS-CoV-2 at moi of 1, and expression of HLA-DR, CD69, CD38, CD27 and PD-1 on MAIT cells, memory CD4⁺ T cells, memory CD8⁺ T cells and γδ T cells was measured 48 h later. Fold change in MFI of HLA-DR, CD69, CD38, CD27 and PD-1 on **(a)** memory CD8⁺ T cells **(b)** memory CD4⁺ T cells **(c)** γδ T cells and **(d)** MAIT cells in virus-infected lung tissue relative to expression on cells from uninfected control cultures is plotted against age (years). Symbols represent individual donors, and the line represents Pearson’s correlation. The dotted line at 1 represents no change in marker expression post-infection. **(e–g)** Cells from whole lung tissue were infected with SARS-CoV-2 at a moi of 1 or mock infected, and at 1, 24 and 48 h later, the amount of viral RNA was measured by RT-qPCR. Each graph depicts the mean (two technical replicates), pooled from two experiments amount of viral RNA (ng μL⁻¹) per donor plotted against **(e)** time or **(f, g)** age (years). **P* < 0.05.

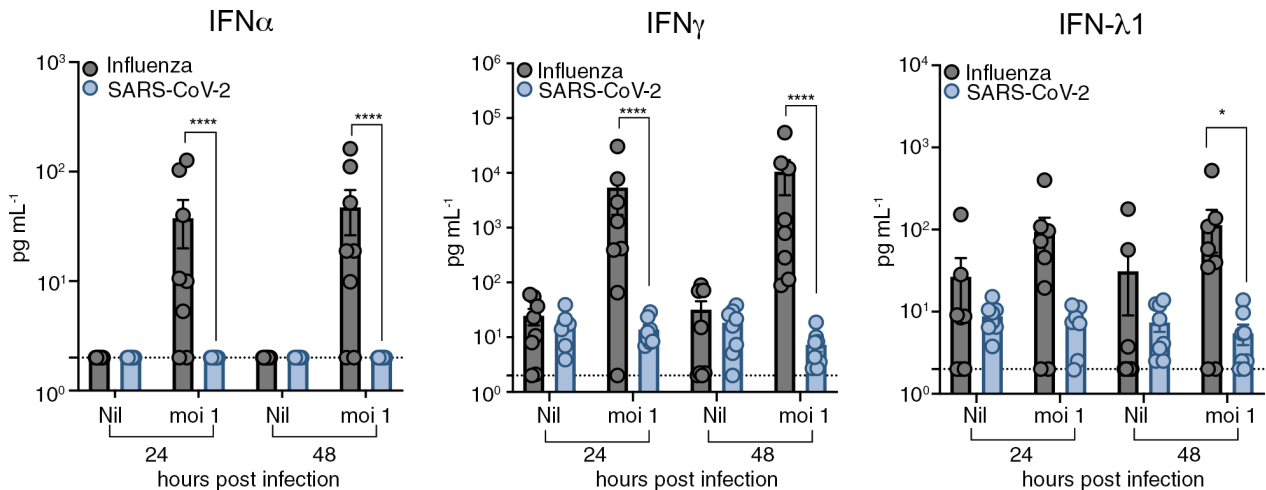


Figure 6. Infection of lung cells with SARS-CoV-2 fails to evoke an early interferon response. Cells from lung tissue were infected with either influenza virus (X31) or SARS-CoV-2 at moi of 1, and the levels of IFN α , IFN γ and IFN λ 1 released into the supernatant at 24 and 48 h were measured using a cytometric bead array. Graphs depict the amount of inflammatory cytokine. Symbols represent individual donors (two-way ANOVA, Sidak's multiple comparison). The dotted line is the limit of detection at 2 pg mL $^{-1}$. * $P < 0.05$; **** $P < 0.0001$.

these cells.²⁴ The half-life of human lung Trm is difficult to define, although elegant studies by Snyder *et al.*,²⁵ tracking CD8 $^{+}$ Trm cells in lung transplant recipients, clearly show the presence of donor-derived passenger CD8 $^{+}$ Trm in the grafted lung for at least 15 months post-transplantation. The age-associated depletion of lung Trm we observed may be driven by the gradual attrition of the human lung Trm pool, which is likely to be occurring throughout life, compounded by an impairment in the ability of older individuals to replenish this memory T-cell subset. Further studies and a larger cohort of clinical samples will be required to fully understand the influence of age on the size of the lung Trm compartment.

Previous clinical studies have shown that the size and quality of the CD8 $^{+}$ T-cell response to the influenza virus decay with age^{26,27} with effector CD8 $^{+}$ T cells in the elderly displaying decreased cytotoxicity against the influenza virus-infected targets.²⁶ In line with these clinical observations, older mice infected with influenza virus initially produced less cytokines and chemokines in the lung, which resulted in a lag in the infiltration of both CD4 $^{+}$ T cells and CD8 $^{+}$ T cells and this, in turn, correlated with delayed viral clearance, prolonged illness and increased mortality rates in the aged cohort.^{28–30} While the development of an effective T-cell response is crucial for the initial clearance of influenza virus infection,^{31,32} the deposition of influenza virus-specific Trm along the airways is key for establishing long-term

heterosubtypic immunity to this pathogen.²³ Mouse models show that pulmonary influenza-specific Trm are indispensable for maintaining heterosubtypic immunity with the loss of this immune subset alone rendering the host susceptible to re-infection.^{23,33,34} Influenza virus-specific Trm are present in human lung tissue,^{9,35} and here, we showed that following exposure to influenza virus, these cells rapidly acquired pro-inflammatory effector functions directly *in situ*. Interestingly, while there does not appear to be any association between the frequency of influenza virus-specific memory CD8 $^{+}$ T cells and donor age, here we observed a change in the memory T-cell subset composition within this virus-specific T-cell pool and found that the proportion of influenza-specific CD8 $^{+}$ Trm cells declined with age. The loss of influenza virus-specific CD8 $^{+}$ Trm that occurred with age coincided with an impaired early antiviral immune response. Thus, the age-associated depletion of influenza virus-specific lung Trm, a key immune cell subset tasked with co-ordinating the early antiviral pro-inflammatory immune response,^{16,18,19} may be yet another factor contributing to the increased susceptibility of the elderly to severe influenza virus disease.

In contrast to influenza virus infection of human lung tissue, which triggered the production of type I, II and III interferon, *in vitro* infection of human lung tissue with SARS-CoV-2 did not evoke an interferon

response. These results are consistent with a recent report by Galani and colleagues who show a diminished early type I and III interferon response in patients hospitalised COVID-19 in contrast to a robust interferon response in patients hospitalised with influenza virus.³⁶ Our findings are also aligned with other studies which show that SARS-CoV-2 replicates covertly in host cells without detectably triggering a type I or III interferon response.³⁷ SARS-CoV-2 expresses multiple viral proteins that perturb signalling pathways both upstream and downstream of interferon production which act to dampen the hosts interferon response.³⁸ As SARS-CoV-2 can outmanoeuvre the innate interferon response, other components of the immune system will need to be recruited to blunt the early stages of infection and restrict viral replication and spread. Our studies infecting human lung tissue with influenza virus show that pathogen-specific CD8⁺ Trm cells in the lung can exert a rapid pro-inflammatory antiviral response following virus exposure. As all tissues in our experiments were banked prior to the emergence of SARS-CoV-2, all donors would have no prior immunity and no local virus-specific T-cell memory in their lung tissue. This is supported by our observation that exposure of lung cells to SARS-CoV-2 did not trigger T-cell activation. Whether infection with SARS-CoV-2 results in the deposition of virus-reactive lung CD8⁺ Trm and whether these cells can orchestrate an effective early antiviral immune response despite the ability of the virus to antagonise the innate interferon response are important questions that will need to be addressed in future studies.

In summary, we observed an age-associated attrition of lung tissue-bound memory CD8⁺ T cells in the elderly. We hypothesise that the loss of the local memory T-cell pool that occurs with advanced age results in an impaired early antiviral immune response which may, in part, explain the increased vulnerability of the elderly to respiratory infections. A better understanding of age-associated changes that occur in the lung immune cell landscape will allow for the development of strategies that boost or preserve tissue-bound memory CD8⁺ T cells, this will enhance local antiviral immune responses and in turn improve the capacity of the elderly to combat respiratory infections.

METHODS

Human lung samples

Lung samples from deceased organ donors were obtained via the Alfred Hospital's Lung Tissue Biobank. As the clinical samples were obtained from organ donors, no data are available on any history of prior influenza virus infections. However, none of the donors died from an influenza virus infection. All organ donors were banked between 2015 and 2019 (Supplementary table 1). Mononuclear cells were isolated and cryopreserved from lungs as previously described.⁹

Ex vivo virus stimulation assay

Stimulation with live virus was performed as described.⁹ Briefly, 2.5×10^5 mononuclear cells from human lung samples were thawed and based on the number of plaque forming units per mL of virus, infected at a multiplicity of infection (moi) of 1 with mouse-adapted x31 influenza A virus (H3N2), influenza virus A/Sydney/203/2000 (H3N2) or influenza virus A/Tasmania/2004/2009 (H1N1pdm09) or SARS-CoV-2 for 1 h at 37°C. Cells were washed and incubated at 37°C in RPMI with 10% foetal calf serum. Cells were stained for expression of activation markers, and supernatants were tested for the presence of a panel of inflammatory cytokines using a LegendPlex Human anti-virus response cytometric bead array (BioLegend). Alternatively, for intracellular cytokine staining experiments, lung cells were infected as described above, washed and incubated at 37°C for 3 h in RPMI with 10% foetal calf serum at which point GolgiPlug (BD Biosciences, San Diego, CA, USA) was added and cells were incubated for a further 18 h. Cells were intracellularly stained for cytokine production.

Flow cytometry

Cells were stained for 1 h on ice with the appropriate mixture of monoclonal antibodies and washed with PBS with 2% BSA. The conjugated mouse and human monoclonal antibodies were obtained from Abcam, BioLegend (San Diego, CA, USA), BD Pharmingen (San Diego, CA, USA), eBioscience (San Diego, CA, USA) or Miltenyi Biotec (see Supplementary table 2). Tetramers were made in house from monomers generously provided by Dr S Gras and Dr J Rossjohn (Monash University, Australia). Tetramer staining was performed at room temperature for 1 h before cell surface staining. Recombinant SARS-CoV-2 RBD-Alexa-647 was made in house. Briefly, recombinant DNA fragments encoding the receptor binding domain (RBD) of SARS-CoV-2 were synthesised (GeneArt Gene Strings, Thermo Fisher Scientific, Waltham, MA, USA) and cloned into the mammalian expression vector pHLSec. RBD-dimer protein was expressed by transient transfection of Expi293S cells using ExpiFectamine 293 Transfection Kits as per manufacturer's instruction (Thermo Fisher Scientific). Protein was purified via protein A, followed by gel filtration size exclusion chromatography using a Superdex-

200 10/300 GL column (Cytiva). Purified RBD-dimer and mouse IgG1 isotype control (clone MOPC-21; BioLegend) were labelled with Alexa Fluor 647 antibody labelling kit (Thermo Fisher Scientific) as per manufacturer's instruction. Specific binding to ACE2 was confirmed by staining 293T.ACE2 cells (Supplementary figure 7) which were generated in house. Briefly, recombinant DNA fragments encoding full-length human ACE2 were synthesised (GeneArt Gene Strings; Thermo Fisher Scientific) and cloned into pMIG. 293T cells were then transiently transfected with pMIG.ACE2 plasmid using FuGENE 6 transfection reagent (Promega). After 48 h, transfected cells were harvested. Cells were stained with RBD-dimer-AF647 or isotype control for 30 min at room temp, washed once and subsequently fixed with 2% PFA for 10 min. Cells were then washed, filtered and transferred to FACS tubes before analysis by flow cytometry using an LSR Fortessa flow cytometer (BD Biosciences).

Lung cells were Fc blocked, stained with $10 \mu\text{g mL}^{-1}$ RBD-dimer-AF647 or isotype control for 30 min, washed once and subsequently fixed with 2% PFA for 10 min. Cells were then washed, filtered and transferred to FACS tubes before analysis by flow cytometry using an LSR Fortessa flow cytometer (BD Biosciences).

RNA extraction and SARS-CoV2 qRT-PCR

All SARS-CoV-2 infection cultures were conducted within the High Containment Facilities in a PC3 laboratory at the Doherty Institute. Stocks of SARS-CoV-2 isolate hCoV-19/Australia/VIC01/2020³⁹ were produced as previously described.⁴⁰ To assess the potential for SARS-CoV-2 to infect and replicate virus genome, cells were pelleted by centrifugation, washed with PBS and pelleted again. The cells were then lysed and viral RNA extracted using the QiaAmp Viral RNA extraction kit (Qiagen, Australia) as per the manufacturer's instructions and stored at -80°C . To evaluate the amount of virus genome present in each sample, a reverse-transcription quantitative PCR (RT-qPCR) for detection of the SARS-CoV-2 envelope (E) gene was performed. Using the SuperScriptIII OneStep RT-PCR System with Platinum[®] Taq DNA Polymerase (Invitrogen, Carlsband, CA, USA), the RT-qPCR assay composed of $5 \mu\text{L}$ RNA, $12.5 \mu\text{L}$ $2\times$ Reaction Master Mix, $0.4 \mu\text{L}$ of 50 mM MgSO_4 , $1 \mu\text{L}$ Superscript III/Taq Enzyme Mix, $0.4 \mu\text{M}$ forward (5'-ACAGGTACGTTAATAGTTAATAGCGT-3'), $0.4 \mu\text{M}$ reverse (5'-ATATTGCAGCAGTACGCACACA-3') primers and $0.2 \mu\text{M}$ primer probe (5'-FAM-ACACTAGCCATCCTTACTGCGC TTCC-BBQ-3'), $1 \mu\text{L}$ of 1 mg mL^{-1} Bovine Serum Albumin (BSA) and $2.6 \mu\text{L}$ RNase-free H_2O . The RT-qPCR assay was performed on a Bio-Rad CFX96 Touch Real-Time PCR Detection System (Bio-Rad, Hercules, CA, USA) using the following conditions: a denaturation step at 55°C for 10 min and 95°C for 3 min, followed by 45 cycles of amplification (94°C for 15 s and 58°C for 30 s). A known amount of SARS-CoV-2 RNA (generated previously from virus stock cultures) diluted twofold was used to generate a standard curve. The Ct values from the standard curve were used to interpolate the amount of SARS-CoV-2 RNA in each sample.

Statistical analysis

Statistical analysis was carried out using GraphPad Prism software (San Diego, CA, USA). One-way or two-way ANOVA was used where appropriate for comparison between two and multiple groups as indicated. Statistical significance was defined to be $*P < 0.05$, $**P < 0.01$, $***P < 0.001$. Pearson correlation analyses were used and r values stated where relevant.

Study approval

Human work was conducted according to the Australian National Health and Medical Research Council Code of Practice. Tissues from deceased organ donors were obtained following written informed consent from the next of kin. The study was approved by the University of Melbourne Human Ethics Committee (ID 1852417 and 1441855).

ACKNOWLEDGMENTS

The University of Melbourne acknowledges the support of Melbourne Health, through its Victorian Infectious Diseases Reference Laboratory at the Doherty Institute, in providing our laboratory with isolated SARS-CoV-2 material. This work was supported by National Health and Medical Research Council of Australia (LMW). KK is supported by Australian NHMRC Investigator Fellowship (#1173871) and the University of Melbourne Dame Kate Campbell Fellowship. THON is supported by NHMRC EL1 Fellowship (#1194036). This study was also supported by the Medical Research Future Fund (#2005544). The Melbourne WHO Collaborating Centre for Reference and Research on Influenza is supported by the Australian Government Department of Health.

CONFLICT OF INTEREST

The authors declare that they have no competing interests.

AUTHOR CONTRIBUTIONS

Julie McAuley: Data curation; Methodology. **Youry Kim:** Data curation. **Glenn Westall:** Methodology. **Thi HO Nguyen:** Data curation; data analysis; methodology. **Ming ZM Zheng:** Data curation; data analysis. **Nicholas A Gherardin:** Resources; data curation; methodology. **Dale I Godfrey:** Resources. **Damian FJ Purcell:** Resources. **Lucy C Sullivan:** Resources. **Patrick C Reading:** Resources. **Katherine Kedzierska:** Resources; supervision. **Linda M Wakim:** Data curation; conceptualisation; supervision; data analysis; writing – original draft.

REFERENCES

1. Lee N, Shin MS, Kang I. T-cell biology in aging, with a focus on lung disease. *J Gerontol A Biol Sci Med Sci* 2012; **67**: 254–263.

2. Chen WH, Kozlovsky BF, Effros RB, Grubeck-Loebenstien B, Edelman R, Szein MB. Vaccination in the elderly: an immunological perspective. *Trends Immunol* 2009; **30**: 351–359.
3. Fulop T, Larbi A, Dupuis G *et al.* Immunosenescence and inflamm-aging as two sides of the same coin: friends or foes? *Front Immunol* 2017; **8**: 1960.
4. Czaja CA, Miller L, Alden N *et al.* Age-related differences in hospitalization rates, clinical presentation, and outcomes among older adults hospitalized with Influenza-U.S. Influenza Hospitalization Surveillance Network (FluSurv-NET). *Open Forum Infect Dis* 2019; **6**: ofz225.
5. Mueller AL, McNamara MS, Sinclair DA. Why does COVID-19 disproportionately affect older people? *Aging (Albany NY)* 2020; **12**: 9959–9981.
6. Gherardin NA, Souter MN, Koay HF *et al.* Human blood MAIT cell subsets defined using MR1 tetramers. *Immunol Cell Biol* 2018; **96**: 507–525.
7. Loh L, Gherardin NA, Sant S *et al.* Human mucosal-associated invariant T cells in older individuals display expanded TCR $\alpha\beta$ clonotypes with potent antimicrobial responses. *J Immunol* 2020; **204**: 1119–1133.
8. Nguyen THO, Sant S, Bird NL *et al.* Perturbed CD8⁺ T cell immunity across universal influenza epitopes in the elderly. *J Leukoc Biol* 2018; **103**: 321–339.
9. Pizzolla A, Nguyen TH, Sant S *et al.* Influenza-specific lung-resident memory T cells are proliferative and polyfunctional and maintain diverse TCR profiles. *J Clin Invest* 2018; **128**: 721–733.
10. Quinones-Parra S, Grant E, Loh L *et al.* Preexisting CD8⁺ T-cell immunity to the H7N9 influenza A virus varies across ethnicities. *Proc Natl Acad Sci USA* 2014; **111**: 1049–1054.
11. Koutsakos M, Illing PT, Nguyen THO *et al.* Human CD8⁺ T cell cross-reactivity across influenza A. *B and C viruses. Nat Immunol* 2019; **20**: 613–625.
12. Pizzolla A, Wakim LM. Memory T cell dynamics in the lung during influenza virus infection. *J Immunol* 2019; **202**: 374–381.
13. Wakim LM, Waithman J, van Rooijen N, Heath WR, Carbone FR. Dendritic cell-induced memory T cell activation in nonlymphoid tissues. *Science* 2008; **319**: 198–202.
14. Park SL, Zaid A, Hor JL *et al.* Local proliferation maintains a stable pool of tissue-resident memory T cells after antiviral recall responses. *Nat Immunol* 2018; **19**: 183–191.
15. Beura LK, Mitchell JS, Thompson EA *et al.* Intravital mucosal imaging of CD8⁺ resident memory T cells shows tissue-autonomous recall responses that amplify secondary memory. *Nat Immunol* 2018; **19**: 173–182.
16. Schenkel JM, Fraser KA, Beura LK, Pauken KE, Vezys V, Masopust D. T cell memory. Resident memory CD8 T cells trigger protective innate and adaptive immune responses. *Science* 2014; **346**: 98–101.
17. Ge C, Monk IR, Pizzolla A *et al.* Bystander Activation of Pulmonary Trm Cells Attenuates the Severity of Bacterial Pneumonia by Enhancing Neutrophil Recruitment. *Cell Rep* 2019; **29**: 4236–4244.e4233.
18. Schenkel JM, Fraser KA, Vezys V, Masopust D. Sensing and alarm function of resident memory CD8⁺ T cells. *Nat Immunol* 2013; **14**: 509–513.
19. Ariotti S, Hogenbirk MA, Dijkgraaf FE *et al.* T cell memory. Skin-resident memory CD8⁺ T cells trigger a state of tissue-wide pathogen alert. *Science* 2014; **346**: 101–105.
20. Purwar R, Campbell J, Murphy G, Richards WG, Clark RA, Kupper TS. Resident memory T cells (TRM) are abundant in human lung: diversity, function, and antigen specificity. *PLoS One* 2011; **6**: e16245.
21. Hombrink P, Helbig C, Backer RA *et al.* Programs for the persistence, vigilance and control of human CD8⁺ lung-resident memory T cells. *Nat Immunol* 2016; **17**: 1467–1478.
22. Slutter B, Braeckel-Budimir N, Abboud G, Varga SM, Salek-Ardakani S, Harty JT. Dynamics of influenza-induced lung resident memory T cells underlie waning heterosubtypic immunity. *Sci Immunol* 2017; **2**: eaag2031.
23. Wu T, Hu Y, Lee YT *et al.* Lung-resident memory CD8 T cells (TRM) are indispensable for optimal cross-protection against pulmonary virus infection. *J Leukoc Biol* 2014; **95**: 215–224.
24. van de Wall S, Badovinac VP, Harty JT. Influenza-specific lung-resident memory CD8⁺ T cells. *Cold Spring Harb Perspect Biol* 2020; a037978.
25. Snyder ME, Finlayson MO, Connors TJ *et al.* Generation and persistence of human tissue-resident memory T cells in lung transplantation. *Sci Immunol* 2019; **4**: eaav5581.
26. Zhou X, McElhaneey JE. Age-related changes in memory and effector T cells responding to influenza A/H3N2 and pandemic A/H1N1 strains in humans. *Vaccine* 2011; **29**: 2169–2177.
27. Yager EJ, Ahmed M, Lanzer K, Randall TD, Woodland DL, Blackman MA. Age-associated decline in T cell repertoire diversity leads to holes in the repertoire and impaired immunity to influenza virus. *J Exp Med* 2008; **205**: 711–723.
28. Toapanta FR, Ross TM. Impaired immune responses in the lungs of aged mice following influenza infection. *Respir Res* 2009; **10**: 112.
29. Quinn KM, Fox A, Harland KL *et al.* Age-related decline in primary CD8⁺ T cell responses is associated with the development of senescence in virtual memory CD8⁺ T cells. *Cell Rep* 2018; **23**: 3512–3524.
30. Jiang J, Fisher EM, Murasko DM. CD8 T cell responses to influenza virus infection in aged mice. *Ageing Res Rev* 2011; **10**: 422–427.
31. van de Sandt CE, Kreijtz JH, de Mutsert G *et al.* Human cytotoxic T lymphocytes directed to seasonal influenza A viruses cross-react with the newly emerging H7N9 virus. *J Virol* 2014; **88**: 1684–1693.
32. Wang Z, Wan Y, Qiu C *et al.* Recovery from severe H7N9 disease is associated with diverse response mechanisms dominated by CD8⁺ T cells. *Nat Commun* 2015; **6**: 6833.
33. Wakim LM, Smith J, Caminschi I, Lahoud MH, Villadangos JA. Antibody-targeted vaccination to lung dendritic cells generates tissue-resident memory CD8 T cells that are highly protective against influenza virus infection. *Mucosal Immunol* 2015; **8**: 1060–1071.
34. Pizzolla A, Nguyen THO, Smith JM *et al.* Resident memory CD8⁺ T cells in the upper respiratory tract prevent pulmonary influenza virus infection. *Sci Immunol* 2017; **2**: eaam6970.

35. Turner DL, Bickham KL, Thome JJ *et al.* Lung niches for the generation and maintenance of tissue-resident memory T cells. *Mucosal Immunol* 2013; **7**: 501–510.
36. Galani IE, Rovina N, Lampropoulou V *et al.* Untuned antiviral immunity in COVID-19 revealed by temporal type I/III interferon patterns and flu comparison. *Nat Immunol* 2021; **22**: 32–40.
37. Park A, Iwasaki A. Type I and Type III interferons – induction, signaling, evasion, and application to combat COVID-19. *Cell Host Microbe* 2020; **27**: 870–878.
38. Lei X, Dong X, Ma R *et al.* Activation and evasion of type I interferon responses by SARS-CoV-2. *Nat Commun* 2020; **11**: 3810.
39. Caly L, Druce J, Roberts J *et al.* Isolation and rapid sharing of the 2019 novel coronavirus (SARS-CoV-2) from the first patient diagnosed with COVID-19 in Australia. *Med J Aust* 2020; **212**: 459–462.
40. Lee JYH, Best N, McAuley J *et al.* Validation of a single-step, single-tube reverse transcription loop-mediated

isothermal amplification assay for rapid detection of SARS-CoV-2 RNA. *J Med Microbiol* 2020; **69**: 1169–1178.

Supporting Information

Additional supporting information may be found online in the Supporting Information section at the end of the article.



This is an open access article under the terms of the Creative Commons Attribution-NonCommercial-NoDerivs License, which permits use and distribution in any medium, provided the original work is properly cited, the use is non-commercial and no modifications or adaptations are made.